

WILEY

An Optical Classification of Coastal and Oceanic Waters Based on the Specific Spectral Absorption Curves of Phytoplankton Pigments, Dissolved Organic Matter, and Other Particulate Materials

Author(s): Louis Prieur and Shubha Sathyendranath

Source: *Limnology and Oceanography*, Jul., 1981, Vol. 26, No. 4 (Jul., 1981), pp. 671-689

Published by: Wiley

Stable URL: <https://www.jstor.org/stable/2836033>

JSTOR is a not-for-profit service that helps scholars, researchers, and students discover, use, and build upon a wide range of content in a trusted digital archive. We use information technology and tools to increase productivity and facilitate new forms of scholarship. For more information about JSTOR, please contact support@jstor.org.

Your use of the JSTOR archive indicates your acceptance of the Terms & Conditions of Use, available at <https://about.jstor.org/terms>



Wiley is collaborating with JSTOR to digitize, preserve and extend access to *Limnology and Oceanography*

JSTOR

An optical classification of coastal and oceanic waters based on the specific spectral absorption curves of phytoplankton pigments, dissolved organic matter, and other particulate materials¹

Louis Prieur and Shubha Sathyendranath

Laboratoire de Physique et Chimie Marines, B.P. 8, La Darse, F 06230 Villefranche sur Mer, France

Abstract

The variations of the spectral absorption coefficient of seawater can be attributed to three principal factors—phytoplankton, nonchlorophyllous particles, and yellow substances—whose concentrations are represented in this study in terms of chlorophyll *a* and pheophytin *a* content (*C*), the total scattering coefficient (*b*), and the absorption by filtered seawater at a given wavelength (*Y*). By assuming an exponential absorption by yellow substances, we developed a new iterative method for identifying the in situ apparent specific spectral absorption curves of the other two factors. The weighting coefficients for each of the three components are calculated for over 80 spectral absorption measurements from different representative marine regions. The reconstruction of spectral absorption curves from the three coefficients and the three specific absorption curves fits the original data with an overall average error of 3%. Relationships between these coefficients and *C*, *b*, and *Y* are examined. Results show that, though the spectral form of absorption by pigments can be considered as more or less invariant, the absorption “efficiency” per unit *C* depends on the nature of the water, and hence on the type of phytoplankton population considered. An optical classification based on the three optical coefficients related to three absorbing agents is proposed.

The absorption coefficient has remained the least studied of the inherent optical properties defined by Preisendorfer (1961), no doubt because of difficulties in its measurement. Along with the volume scattering function and the total volume scattering coefficient, it is however an important parameter which describes the influence of dissolved and suspended matter on the propagation of electromagnetic waves in water. It is indispensable for characterizing an optical medium in all model studies on radiative transfer. Inversely, it is a necessary intermediary—implicit or explicit—in all indirect evaluations of the nature and quantities of these substances from certain apparent optical properties, often more easily measurable, including diffuse reflectance and the diffuse attenua-

tion coefficient. Diffuse reflectance, the spectral variations of which determine the color of the sea, is very much studied currently because of its applications in remote sensing. The diffuse attenuation coefficient determines the decrease with depth of the energy available for photosynthesis.

Three groups of substances are generally considered responsible for significant modifications of the absorbing properties of seawater: phytoplankton, nonchlorophyllous particles of biologic or terrestrial origin, and dissolved organic matter (also known as yellow substances). Therefore, the total absorption coefficient *a* (m⁻¹), observed at any given wavelength λ , can be expressed, if fluorescence effects be neglected, as

$$a(\lambda) - a_w(\lambda) = Ca_c^*(\lambda) + Pa_p^*(\lambda) + Ya_y^*(\lambda). \quad (1)$$

a_w is the absorption by pure seawater, practically the same as that of pure water in the visible region (400–700 nm), which is studied here. Absorption by dissolved salts is known to be negligible in this re-

¹ The data on which this study is based were acquired with the assistance of CNRS (contracts RCP 247 and ERA 278), and the study was supported in part by CNEXO (contract 77/1695 and 79/2010) and in part by CNES (contract 79/250). This study is a contribution to the work initiated by the IAPSO Working Group on Optical Oceanography.

gion. The absorption related to each group of substances is expressed as a product of its concentration C , P , or Y and the corresponding specific absorption a_c^* , a_p^* , or a_y^* (m^{-1} per unit concn).

Each group is in fact constituted of several substances, often present in differing proportions, and, as their absorbing properties are slightly different, the specific absorption curve of each group is subject to a certain variability, which is neglected here. To facilitate practical applications, we propose that the concentrations of each group be indicated by routinely measurable parameters. Concentration of chlorophyll a and pheophytin a (C , $\text{mg} \cdot \text{m}^{-1}$) is used here as a measure of the concentration of phytoplankton and its immediate derivatives or by-products having similar optical effects. Concentration of nonchlorophyllous particles (P , m^{-1}) is given in terms of the total scattering coefficient b , and the concentration of yellow substances (Y , m^{-1}) in terms of absorption by filtered water measured at a chosen wavelength.

Spectral variations of absorption by yellow substances are known at least in relative units. Our aim in this study is to find the specific absorption curves related to C and P by a particular method making use of all our data on the spectral values of absorption coefficient obtained from in situ measurements. A classification based on three partial absorption coefficients related to C , P , and Y is then proposed. Some applications of the results in simple modeling of the spectral values of absorption coefficient and the penetration of light in seawater are discussed.

We thank A. Morel for help and encouragement in the course of this work, and L. Legendre for comments on the manuscript.

Data

Optical data—We used 90 sets of spectral values of absorption coefficient made at 5-nm intervals from 400 to 700 nm for seawater in various regions. The absorption values were calculated for the surface layer from the values of upwelling

(E_u) and downwelling (E_d) irradiance and the sun zenith angle in water, j . Irradiance was measured with an underwater spectroirradiance meter (Bauer and Ivanoff 1970). The values of the absorption coefficient a at wavelength λ were deduced from the expression (Morel and Prieur 1975)

$$a(\lambda) = \frac{K_d(\lambda)[1 - R(\lambda)]\cos j}{0.6 + [0.47 + 2.5R(\lambda)]\cos j}. \quad (2a)$$

The derivation of the equation which contains some approximations is briefly recalled.

The law of conservation of energy can be expressed as

$$\frac{d(E_d - E_u)}{dz} = -a(z)E_0(z) \quad (2b)$$

for radiant energy of a given wavelength, in a stratified medium at depth z , where E_0 is the scalar irradiance. Equation 2b is easily transformed as

$$a(z) = K_d(z) \left[1 - R(z) + \frac{1}{K_d} \frac{dR(z)}{dz} \right] \frac{E_d(z)}{E_0(z)} \quad (2c)$$

where $K_d(z) = -d \ln E_d(z)/dz$ is the diffuse attenuation coefficient for downwelling irradiance and $R = E_u/E_d$ is diffuse reflectance. The ratio $E_d:E_0$ can be expressed as

$$\frac{E_d}{E_0} = 1 / \left[\frac{1}{\bar{\mu}_d} + \frac{R(z)}{\bar{\mu}_u} \right] \quad (2d)$$

where $\bar{\mu}_d$ and $\bar{\mu}_u$ are the mean cosines for the downwelling and upwelling irradiance fields. These transformations of Eq. 2b, which are without any approximation, have been given by Preisendorfer (1961) and Pelevin (1965).

K_d and R could be calculated directly by using our measurements of upwelling and downwelling irradiance. The term $(1/K_d)[dR(z)/dz]$ could also be calculated from the measurements at our disposal by using the relationship

$$K_d - K_u = \frac{1}{R} \frac{dR}{dz}.$$

Since R , as well as $(K_d - K_u)$ are only small fractions of one, the term $R(K_d -$

$K_u)/K_d$ can be safely neglected. But the calculation of a requires two approximations. $\bar{\mu}_d$ and $\bar{\mu}_u$ are not measured and ought to be evaluated indirectly. For diverse radiant fields and depths, $1/\bar{\mu}_u$ varies at the most from 2.3 to 3 (Priour and Morel 1971; Tyler and Preisendorfer 1962; Pelevin 1965). The constant value adopted here is 2.5. In Eq. 2d, $1/\bar{\mu}_u$ is multiplied by R and the variations due to $1/\bar{\mu}_u$ can therefore reasonably be neglected. Some workers (Pelevin 1965; Højerslev 1974) take $\cos j$ for $\bar{\mu}_d$. A more precise estimation of $1/\bar{\mu}_d$ for the surface layer is given by

$$\frac{1}{\bar{\mu}_d} = \frac{0.6}{\cos j} + \frac{0.4}{0.859}$$

which represents a weighting of the influence of direct sunlight $1/\cos j$ and of sky light $1/0.859$. The weighting factors 0.6 and 0.4, estimated from the results of Sauberer and Ruttner (1941), do not have a great influence on the resultant value of $\bar{\mu}_d$ because $\cos j$ varies from 1 ($h_0 = 90^\circ$) to 0.71 ($h_0 = 20^\circ$) for our data, and are therefore never very different from 0.859. In the case of an overcast sky, $\bar{\mu}_d$ is taken equal to 0.859, the value corresponding to a cardioidal distribution of radiance. Actually, the contributions of sunlight and sky light to the total irradiance depend on wavelength. The possible variations of $\bar{\mu}_d$ between the extremes of 400 and 700 nm can be evaluated at 7%. The relative uncertainty of a at the extreme wavelengths is therefore of this order.

Equation 2c is established for a depth Z . K_d could only be calculated here between two depths, 0_+ just above water and Z , a depth sufficiently great for the fluctuations of irradiance introduced due to sea roughness to be negligible. Consequently, Z varies from 4 to 20 m depending on the clarity of the water. Absorption in this surface layer is supposed to be constant. K_d is therefore evaluated by

$$K_d = \frac{1}{Z} \ln \frac{E(0_+)}{E(z)}.$$

R is taken as the ratio of the upwelling

irradiance just below the surface (at a depth <1 m) to $E(0_+)$. Equation 2a is easily derived from Eq. 2c, taking into account the approximations for $\bar{\mu}_d$, $\bar{\mu}_u$, and K_d .

Other data—The following data were also used whenever available. b : total scattering coefficient at 550 nm measured with a scatterance meter (Bauer and Ivanoff 1971); Y : absorption by filtered water at 440 nm, either measured directly or calculated from measurements at other wavelengths; C : concentration of chlorophyll a and pheophytin a measured in acetone extracts.

Table 1 gives the number of observations of these data during the different cruises, the areas, and the types of water. These data constitute a reasonably good sampling of the diverse types of marine environment, covering the range from the oligotrophic waters of the Sargasso Sea to the turbid or productive waters of coastal upwelling zones. The Emericort and Fos-Berre stations represent a very special case of waters highly polluted by domestic and industrial discharges and are included only for comparison with truly marine systems.

Method

When we consider the terms of Eq. 1, $a_w(\lambda)$ and $a_y(\lambda)$ can be taken as parameters known with sufficient accuracy. The values of $a_w(\lambda)$ used here are those given by Morel and Priour (1977) (see Table 2 and Fig. 1). Absorption by yellow substances varies exponentially with wavelength (Kalle 1966; Kirk 1976b; Højerslev 1974; Jerlov 1976). Morel and Priour (1976) expressed this variation as

$$a_y(\lambda) = a_y(\lambda_0) \exp[-0.014(\lambda - \lambda_0)] \quad (3)$$

where $a_y(\lambda)$ and $a_y(\lambda_0)$ are absorption by filtered water at wavelengths λ and λ_0 . Bricaud (1979) studied 105 samples from various regions and showed that the value of the exponential coefficient, though not strictly invariable, is centered around -0.014 (SD = 0.003). We accept it as a constant for this study.

For the stations where the values of C , Y , and P are known along with $a(\lambda)$, a

Table 1. Data used in this study. Cruises, dates, zones studied, and description of zones are given, along with the number of observations of spectral values of absorption (*a*) and corresponding measurements of scattering coefficient (*b*), pigment concentration (chlorophyll *a* + pheophytin *a* = *C*), and absorption by yellow substances (*Y*).

Cruise	Date	Zone	Type of zone	No. available observations*			
				<i>a</i>	<i>b</i>	<i>C</i>	<i>Y</i>
Discoverer	May 70	Central E. Pacific, Sargasso Sea, Gulf of Mexico	Oceanic	11(a)	11(b)	11(e)	—
Cineca II	Apr 71	Off Mauritania	Coastal upwelling	4(a)	4(b)	—	—
Harmattan	May 71	Off Liberia and Ivory Coast	Turbid nearshore	1(a)	—	—	—
			Offshore	8(a)	—	—	—
Cineca V	Apr 74	Off Mauritania	Turbid nearshore	12(a)	5(c)	5(f)	3(h)
			Offshore upwelling	35(a)	17(c)	19(f)	6(h)
Antiprod	Mar 77	Indian Antarctic	Clear oceanic	9(b)	9(d)	9(g)	—
Fos-Berre	May 77	Off Marseilles	Very turbid urban coastal	5(b)	3(b)	4(b)	4(b)
Emicort	Dec 77	Off Marseilles	Very turbid urban coastal	6(b)	—	6(b)	6(b)

* (a) Morel and Prieur 1975; (b) Morel and Prieur unpubl.; (c) Prieur and Morel 1976; (d) Morel and Prieur 1978; (e) Baird 1973, (f) Jacques et al. 1976; (g) Jacques 1978; (h) Morel and Prieur 1976.

regression method would permit estimation of $a_c^*(\lambda)$ and $a_p^*(\lambda)$ (Prieur 1976; Morel and Prieur 1977). But this method is limited because the values of *C*, *Y*, and *P* are not known to the precision necessary for such a calculation at all stations, for several reasons: the inherent imprecision of individual measurements is not negligible; there is no exact concordance between times of measurements of irradiance, *C*, *Y*, and *P*; and $a(\lambda)$ values are in fact mean values for the surface layer, while *C*, *Y*, and *P* are obtained at one or several discrete levels near the surface, which could introduce a discrepancy in the data if the layer were not homogeneous.

In the present method we try to minimize the importance of the individual errors in estimating *C*, *P*, and *Y* by considering principally the whole set of spectral data. At the same time, we try to find component curves that can be interpreted easily from a physical point of view and that can be used in reconstructing the spectral absorption curve with a good fit. The method is based on forms of the spectral absorption curves.

Identification of typical forms—Three recurring typical forms are shown in Fig. 1. The V-form (Fig. 1A) and the U-form (Fig. 1B) have been defined by Morel and Prieur (1977) and the spectral char-

acteristics of the corresponding irradiance attenuation curves described by Morel (1981). Briefly, while the chlorophyll absorption peaks at 440 and 675 nm, the pheophytin peak at 410 nm and the carotenoid shoulder at 480 nm combine to give the characteristic shape to the curves in Fig. 1A, these effects are not noticeable in the curves of Fig. 1B. The V-type stations are those aligned along the X-axis in Fig. 2, and the U-type stations are those aligned along the Y-axis. In other words, the main absorbing factors are related to *C* in the case of the V-type stations and to *b* in the case of the U-type stations. A third type of station should correspond to predominant absorption by yellow substances. Such curves (the reversed J-type) are shown in Fig. 1C. Often, intermediate cases are observed with more than a single major absorbing agent; two examples are shown by dashed lines in Fig. 1A, B.

Normalization—Each of the characteristic specific absorption curves, normalized to its respective value at 440 nm, is considered. They are represented by $a_c^{*'}(\lambda)$, $a_y^{*'}(\lambda)$, and $a_p^{*'}(\lambda)$, and their corresponding coefficients by *C'*, *Y'*, and *P'* so that (from Eq. 1)

$$a_i(\lambda) = C_i' a_c^{*'}(\lambda) + Y_i' a_y^{*'}(\lambda) + P_i' a_p^{*'}(\lambda)$$

(4a)

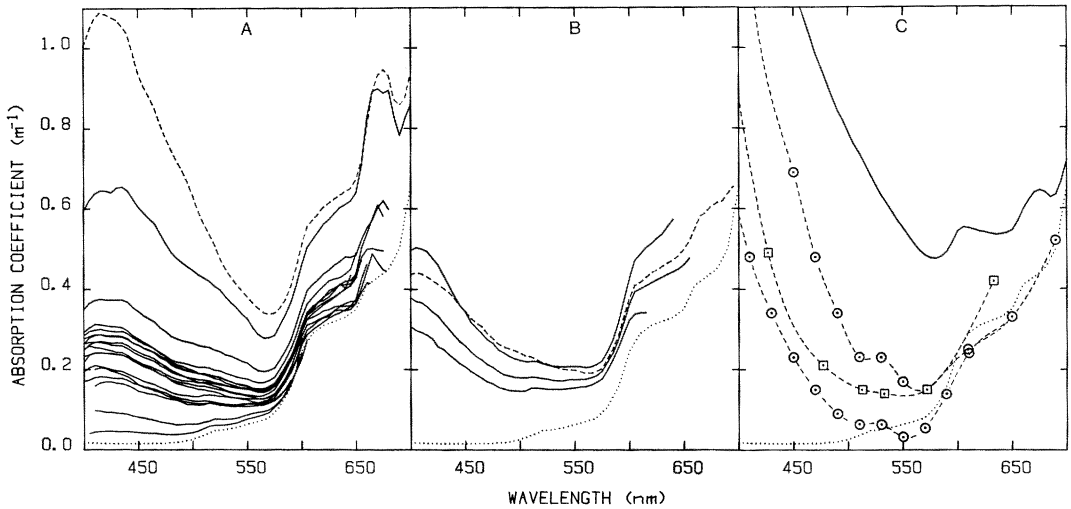


Fig. 1. Typical forms of spectral absorption curves (solid lines), compared to that of pure water (dotted lines). A. V-type. For these stations Chl + Pheo (= C) concentrations vary from 0.2 to 18.4 $\text{mg} \cdot \text{m}^{-3}$ and total scattering coefficient b from 0.16 to 1.5 m^{-1} . An intermediate case is represented by station 3 of Fosse-Berre (dashed line) where, in addition to C , yellow substances also probably absorb significantly. B. U-type. C values are almost the same at these stations ($\approx 2 \text{ mg} \cdot \text{m}^{-3}$) but scattering coefficient varies from 1.55 to 3.6 m^{-1} . Station 47 of Cineca V (dashed line) is an intermediate case between U- and V-types ($C = 6.4 \text{ mg} \cdot \text{m}^{-3}$, $b = 2.5 \text{ m}^{-1}$). C. Reversed J-type (or J-type). Only one of our stations (—) among data recently obtained from waters around Vancouver Island represents this type. But other measurements at discrete wavelengths exhibit the same form (Højerslev 1974: \square ; Kopelevich et al. 1974: \circ). Some values are lower than absorption by pure water, probably due to lack of precision in absolute values, but forms of the curves seem reliable.

and

$$a_i(440) = C_i' + Y_i' + P_i'. \quad (4b)$$

For the sake of simplicity, $a(\lambda)$ stands for $[a(\lambda) - a_w(\lambda)]$ here and henceforth, unless otherwise noted. The subscript i stands for station. It is evident that, by virtue of the normalization, $a_c^{*'}(\lambda)$, $a_y^{*'}(\lambda)$, and $a_p^{*'}(\lambda)$ are now all dimensionless, and their coefficients have units of m^{-1} .

Now, C_i' , Y_i' , P_i' for each station and mean $a_c^{*'}(\lambda)$ and $a_p^{*'}(\lambda)$ must be determined from the whole set of spectral absorption coefficients.

Calculation of $a_c^{*'}(\lambda)$ and $a_p^{*'}(\lambda)$ —Mean $a_c^{*'}(\lambda)$ and $a_p^{*'}(\lambda)$ are determined by an iterative calculation on U and V forms, described in Fig. 3. The equations used are combined forms of Eq. 4a (or 4b) and its derivative at 440 nm. X_i and Z_i are intermediate quantities introduced to facilitate the presentation. The scheme was drawn on the basis that a set of stations at which Y_i' and P_i' equal zero does not

exist. In particular, absorption by yellow substance is never negligible even at stations very rich in phytoplankton. But for the V-type stations, P' could be considered negligible in a first approximation. We then calculated $a_c^{*'}(\lambda)$ for each V-type station and each wavelength after giving one value to $(\delta a_c^{*'} / \delta \lambda)_{440}$. As the absorption coefficient of chlorophyll a in vivo has a maximum near 440 nm, the first value introduced was zero. But the presence of other pigments in variable proportions, notably carotenoids and pheophytin, could shift the maximum of phytoplankton absorption from 440. The final value of $(\delta a_c^{*'} / \delta \lambda)_{440}$ was determined by trial and error to be that value which minimized dispersion among the individual $a_c^{*'}(\lambda)$ curves while all values of C_i' and Y_i' were nonnegative. Mean $a_c^{*'}(\lambda)$ was then calculated and introduced in the calculation of $a_p^{*'}(\lambda)$ using three U-type stations where C was about the same as that at station 70 of Cineca 5, one of the V-

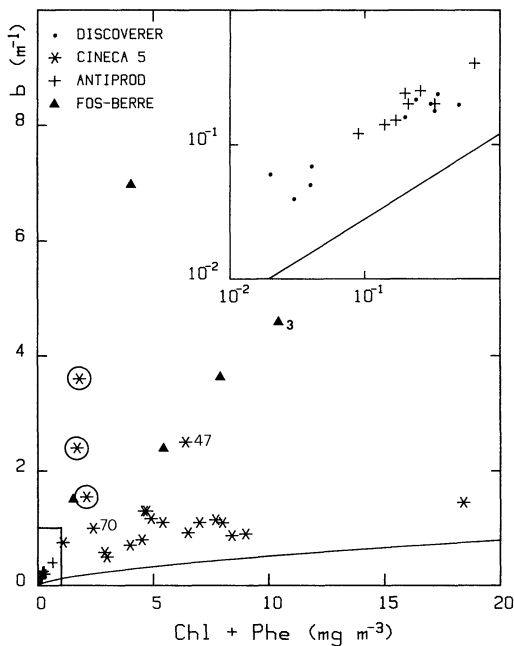


Fig. 2. Plot of scattering coefficient b vs. concentration of Chl + Pheo ($= C$) for diverse stations. Different cruises identified by different symbols. Stations with very small values of b and C in rectangle on lower left are plotted in inset on upper right on a log-log scale. Line represents Eq. 8. Stations nearest line are V-type stations. U-type stations (given in Fig. 1B) are circled. Stations 47 and 70 of Cineca V and station 3 of Fos-Berre identified by their numbers.

type stations (see Fig. 2). The chlorophyll absorption, assumed to be the same and equal to $C_{70}'a_c^{*'}(\lambda)$, was then subtracted to calculate Z_i . Once we obtained mean $a_p^{*'}(\lambda)$, we calculated C_i' , Y_i' , and P_i' by multiple regression on $a_c^{*'}(\lambda)$, $a_y^{*'}(\lambda)$, and $a_p^{*'}(\lambda)$ for all V-type stations. This procedure was then repeated, now introducing the previously obtained values of P_i' $a_p^{*'}(\lambda)$ into the calculations of $a_c^{*'}(\lambda)$. P_i' values were generally small.

Successive results became identical by the end of the fifth cycle, with $(\delta a_c^{*'} / \delta \lambda)_{440} = -0.03$, $(\delta a_p^{*'} / \delta \lambda)_{440} = -0.0205$, and $C'_{70} = 0.117 \cdot m^{-1}$. The form of the $a_p^{*'}(\lambda)$ curve was not very sensitive to small changes introduced in the value of C'_{70} . The final estimates of mean $a_c^{*'}(\lambda)$ and $a_p^{*'}(\lambda)$ as well as $a_y^{*'}(\lambda)$ are shown in Fig. 4. $a_p^{*'}(\lambda)$ could only be calculated

up to 605 nm as absorption values at higher wavelengths were not available for two of the three selected U-type stations. The dotted line extending from 605 to 700 nm indicates values given by a single station and used in the iterations. Table 2 presents the values of $a_w(\lambda)$, $a_y^{*'}(\lambda)$, $a_c^{*'}(\lambda)$, and $a_p^{*'}(\lambda)$.

Calculation of the coefficients C' , Y' , P' and A by ridge regression—A few of the curves that closely resembled that of pure water were eliminated from the data as they evidently contained very little particulate or dissolved matter and their coefficients could therefore be considered to be zero. The coefficients C' , Y' , P' were then calculated by multiple regression for all remaining stations. No condition was imposed that the constant coefficient, say A , of the multiple regression be equal to zero. Spectral absorption values from 400 to 570 nm (35 wavelengths) only were used. Higher values were omitted for the following reasons. First, beyond 570 nm, $a_w(\lambda)$ increases rapidly with increasing wavelength and small errors in calculating total absorption could result in a significant error in $|a_i(\lambda) - a_w(\lambda)|$. Second, beyond 600 nm, errors of measurement increase because the sensitivity of the spectro-irradiance meter is lower in this region. Third, the absorption values at greater wavelengths were not known for all the stations, and in this study we wanted to keep the upper limit of calculation the same for all the stations.

The least-squares estimates sometimes had negative signs and unexpected magnitudes. As this could be the effect of correlation between independent variables, this problem was overcome by the method of ridge regression (see Hoerl and Kennard 1970a,b; Marquardt 1970; Jones 1972). The coefficients so obtained are biased, but have the advantage of stability. The technique of ridge regression was also used in previous successive iterations to modify the coefficient P' obtained by the classical least-squares method.

Figure 5 presents the original observed spectral absorption values and the curves constructed by using the four coefficients

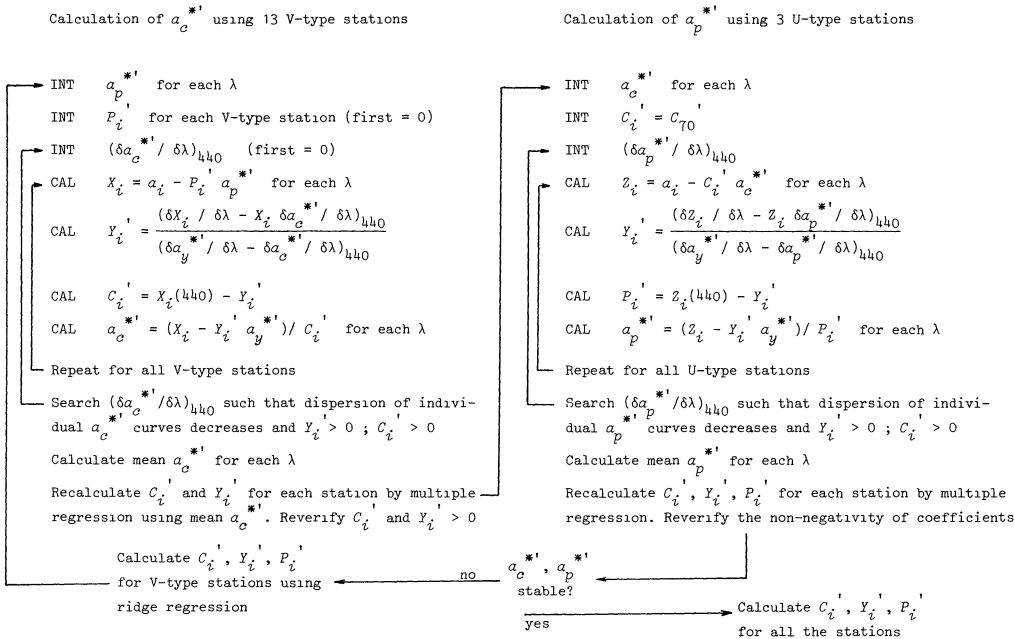


Fig. 3. Scheme of calculating $a_c^{*'}(\lambda)$ and $a_p^{*'}(\lambda)$. CAL and INT stand for calculate and introduce.

and the characteristic curves for six stations. The relative error of the reconstructed curve was estimated as

$$\Sigma |a_i(\lambda)_{\text{meas}} - a_i(\lambda)_{\text{calc}}| \Delta \lambda / \Sigma a_i(\lambda)_{\text{meas}} \Delta \lambda.$$

On average, this error was 1.3% (max 3.2%) when the error was calculated only up to 570 nm. As expected, the error increased noticeably when reconstructed values beyond 570 nm were also considered (mean error 4.6%, max 15.5%). The good reconstruction of all curves

Table 2. Spectral values of absorption coefficient of pure water (a_w) and normalized spectral absorption values of phytoplankton pigments ($a_c^{*'}$), nonchlorophyllous particles ($a_p^{*'}$), and yellow substances ($a_y^{*'}$).

λ	a_w	$a_c^{*'}$	$a_p^{*'}$	$a_y^{*'}$	λ	a_w	$a_c^{*'}$	$a_p^{*'}$	$a_y^{*'}$	λ	a_w	$a_c^{*'}$	$a_p^{*'}$	$a_y^{*'}$
400	0.018	0.687	1.892	1.751	500	0.026	0.668	0.473	0.432	600	0.245	0.236	0.850	0.106
405	0.018	0.781	1.766	1.632	505	0.031	0.645	0.480	0.403	605	0.268	0.279	0.913	0.099
410	0.017	0.828	1.726	1.522	510	0.036	0.618	0.509	0.375	610	0.290	0.252	0.879	0.093
415	0.017	0.883	1.635	1.419	515	0.042	0.582	0.495	0.350	615	0.300	0.268	0.877	0.086
420	0.016	0.913	1.534	1.323	520	0.048	0.528	0.488	0.326	620	0.310	0.276	0.875	0.080
425	0.016	0.939	1.410	1.234	525	0.050	0.504	0.488	0.304	625	0.315	0.299	0.910	0.075
430	0.015	0.973	1.274	1.150	530	0.051	0.474	0.495	0.284	630	0.320	0.317	0.935	0.070
435	0.015	1.001	1.119	1.073	535	0.054	0.444	0.505	0.264	635	0.325	0.333	0.992	0.065
440	0.015	1.000	1.000	1.000	540	0.056	0.416	0.526	0.247	640	0.330	0.334	1.041	0.061
445	0.015	0.971	0.914	0.932	545	0.060	0.384	0.548	0.230	645	0.340	0.326	1.133	0.057
450	0.015	0.944	0.868	0.869	550	0.064	0.357	0.548	0.214	650	0.350	0.356	1.227	0.053
455	0.016	0.928	0.764	0.811	555	0.068	0.321	0.566	0.200	655	0.380	0.389	1.337	0.049
460	0.016	0.917	0.691	0.756	560	0.071	0.294	0.565	0.186	660	0.410	0.441	1.528	0.046
465	0.016	0.902	0.636	0.705	565	0.076	0.273	0.587	0.174	665	0.420	0.534	1.542	0.043
470	0.016	0.870	0.589	0.657	570	0.080	0.276	0.599	0.162	670	0.430	0.595	1.542	0.040
475	0.017	0.839	0.567	0.613	575	0.094	0.268	0.569	0.151	675	0.440	0.544	1.542	0.037
480	0.018	0.798	0.522	0.571	580	0.108	0.291	0.624	0.141	680	0.450	0.502	1.542	0.035
485	0.019	0.773	0.496	0.533	585	0.133	0.274	0.649	0.131	685	0.475	0.420	1.542	0.032
490	0.020	0.750	0.483	0.497	590	0.157	0.282	0.718	0.122	690	0.500	0.329	1.542	0.030
495	0.023	0.717	0.474	0.463	595	0.201	0.249	0.805	0.114	695	0.575	0.262	1.542	0.028
										700	0.650	0.215	1.542	0.026

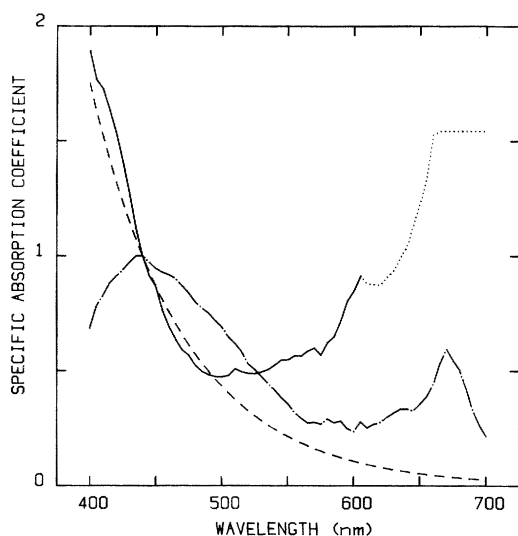


Fig. 4. Normalized specific absorption curves of chlorophyllous pigments $a_c^*(\lambda)$ (— · — · —) and nonchlorophyllous particles $a_p^*(\lambda)$ (—) in suspension in seawater (this study). Absorption curve of yellow substance $a_y^*(\lambda)$ (· · · · ·) used here is also presented. Curves normalized at 440 nm. Validity of dotted part of $a_p^*(\lambda)$ curve is questionable because it is based on a single station.

shows that spectral information can be condensed into four coefficients, three of them being the weightings of the three normalized absorption curves and the fourth being independent of wavelength.

Relationships between calculated coefficients and measured parameters—The partial absorption coefficients C' , Y' , P' , and A were determined only from the spectral data. We now examine the significance of the coefficients by studying correlations between observed parameters and these calculated partial absorption coefficients.

The relationship between C' and C are different for different types of waters. As can be seen from Fig. 6A, the relationships between C' and C are remarkably different for clear oceanic waters (Discoverer and Antiprod stations with $C < 1 \text{ mg} \cdot \text{m}^{-3}$) and the more productive waters of the west coast of Africa (Cineca stations; see also Fig. 2). So, we fitted two separate equations to the data, which gave the following relations:

$$C'(\text{m}^{-1}) = 0.008 + 0.070C(\text{mg} \cdot \text{m}^{-3}) \quad (5a)$$

for $C < 1 \text{ mg} \cdot \text{m}^{-3}$ with $r = 0.84$ and $n = 13$, and

$$C'(\text{m}^{-1}) = 0.058 + 0.018C(\text{mg} \cdot \text{m}^{-3}) \quad (5b)$$

for $C > 1 \text{ mg} \cdot \text{m}^{-3}$ with $r = 0.94$ and $n = 27$. These equations give 0.078 and 0.076 as the value of C' when C is one; we have taken the value of C' to be 0.077 at this point of discontinuity. Such a discon-

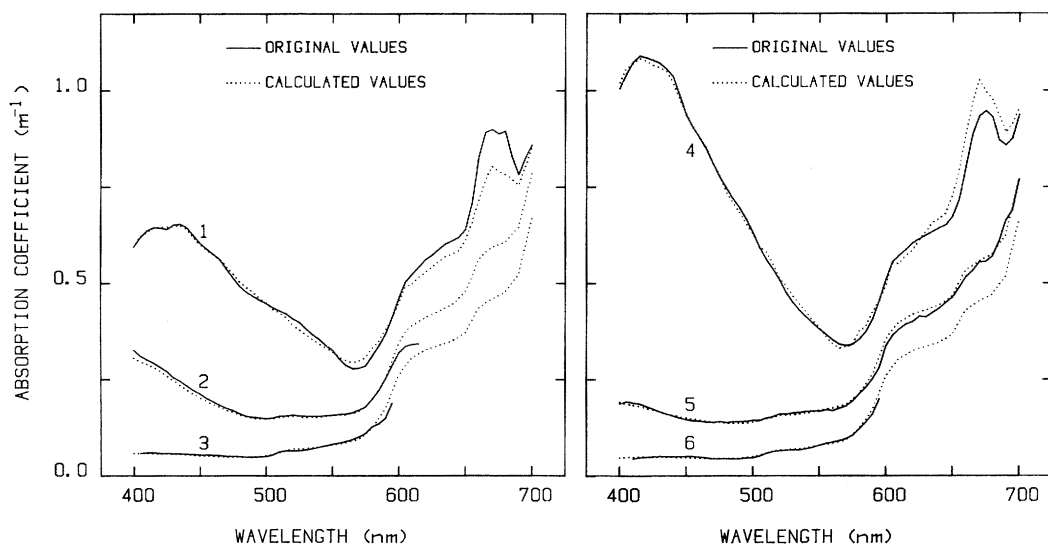


Fig. 5. Six examples of original and calculated curves for comparison. 1—Station 71, Cineca V; 2—station 47, Cineca V; 3—station 10, Discoverer; 4—station 2, Fos-Berre; 5—station 3, Emicort; 6—station 24, Antiprod.

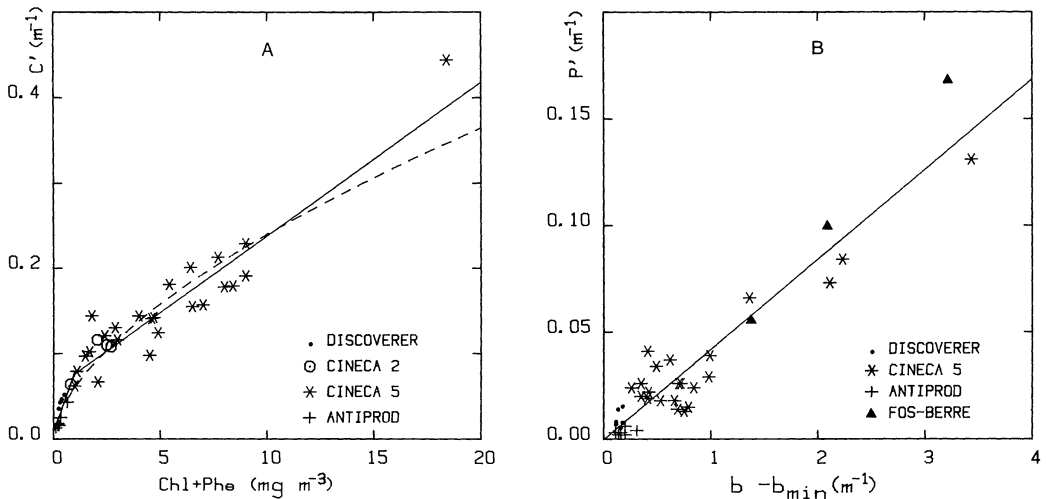


Fig. 6. Relationship between C' and C , and P' and P . A. Scatter diagram of C' and $\text{Chl} + \text{Pheo}$ ($= C$) for Discoverer, Cineca II, Cineca V, and Antiproduct cruises. Solid line with discontinuity at $C = 1 \text{ mg} \cdot \text{m}^{-3}$ represents Eq. 5a and b. Dashed line represents Eq. 5c. B. Scatter diagram of P' and $b - b_{\min}$ ($= P$). Line plotted is given by Eq. 8.

tinuity in the relationship between optical properties and pigment concentrations has been pointed out by Smith and Baker (1978a), who considered the discontinuity to be the effect of variations in the relative importance of other biogenous material coexisting with the phytoplankton. But even after we take into account, at least to a certain extent, the effects of yellow substance and nonchlorophyllous particles, the discontinuity persists here. This suggests that it could be due to changes in the relative importance of other pigments in the phytoplankton population, or to a change in the "absorption efficiency" of the live pigments which probably accompanies a change in the population and their physiological state, or to a combined effect of these phenomena. The data on which Eq. 5a and b are based can in fact be represented equally well by the single relationship:

$$C'(\text{m}^{-1}) = 0.06 [C(\text{mg} \cdot \text{m}^{-3})]^{0.602} \quad (5c)$$

with $r = 0.96$ for the logarithmic values and $n = 40$. The higher correlation coefficient of this curve suggests that the change in the rate of absorption per unit C is gradual, rather than abrupt. But Eq. 5c seems to underestimate C' more than

does Eq. 5b for very high concentrations of C (of the order of $20 \text{ mg} \cdot \text{m}^{-3}$).

Equations 5a, b, and c do not increase the accuracy of estimating C from the optical data over the much simpler relation proposed by Morel (1980: fig. 6) between C and the blue-green ratio of diffuse reflectance. The advantage of the equations presented here, which are based on absorption, is that they are also applicable to the turbid inshore upwelling waters of the west coast of Africa which Morel considered as a case apart.

Equation 5d represents eutrophic waters influenced by proximity of the city and port of Marseilles.

$C'(\text{m}^{-1}) = 0.017 + 0.077C(\text{mg} \cdot \text{m}^{-3}) \quad (5d)$
for $0 < C < 12 \text{ mg} \cdot \text{m}^{-3}$, with $r = 0.97$ and $n = 10$. It is remarkable how closely this resembles Eq. 5a, which is applicable to open ocean waters with low concentrations of particulate and dissolved matter.

Part of the total scattering is due to phytoplankton, i.e. related to the parameter C . This part of the scattering, b_{\min} (at $\lambda = 550 \text{ nm}$), can be estimated by the relationship given by Morel (1980):

$$b_{\min}(\text{m}^{-1}) = 0.12 [C(\text{mg} \cdot \text{m}^{-3})]^{0.63} \quad (6)$$

(see Fig. 2). This relationship was de-

duced from the scatter diagram of b and Chl + Pheo, as the minimum scattering observed for a given Chl + Pheo. We then define

$$P(m^{-1}) = (b - b_{min})(m^{-1}) \tag{7}$$

where P represents the concentration of nonchlorophyllous particles. P is plotted against P' in Fig. 6B. A linear best-fit gave the equation

$$P'(m^{-1}) = -0.00029 + 0.42P(m^{-1}) \tag{8}$$

with $r = 0.95$ and $n = 39$. The regression is based on data from Discoverer, Cineca V, and Antiprod, as well as Fos-Berre.

Comparison of Y' with the few values of Y available showed a high dispersion. This dispersion can probably be explained by the storage of water samples before absorption was measured in the laboratory. Bricaud (1979) pointed out that storage affects the absolute values of $a_y(\lambda)$, although its influence on its exponential coefficient (*see Eq. 3*) would be less pronounced. In addition, Y' is a measure of all substances, particulate or dissolved, whose absorption curve is exponential, whereas Y is a measure of the dissolved portion. The presence of yellow substances in colloidal or adsorbed form would thus complicate the relationship between Y' and Y . Also, different procedures had been used to obtain the Y values in our data. A standardized method of measuring absorption by yellow substances needs to be defined. Changing the exponential coefficient within the range observed by Bricaud (1979) did not alter the values of Y' enough to explain the discrepancy between the measured and observed parameters.

According to Eq. 2, coefficient A ought to have been zero. In fact, the value of A is low in general, but is nonnegligible at times. This coefficient does not show any significant relationship with any other coefficients or measured parameters (*see Table 3*). An error in the estimate of the depth interval Z over which the diffuse attenuation K is calculated can introduce an offset, positive or negative, in the absorption coefficient $a(\lambda)$. A statistical

Table 3. Table of correlation coefficients between optical coefficients (C' , Y' , P' , and A) and measured parameters (C , Y , and P).

	C'	Y'	P'	A
C $n = 49$	0.718	0.498	0.114	0.110
Y $n = 19$	0.239	0.659	0.543	0.521
P $n = 37$	0.606	0.843	0.951	0.281

study of the influence of Z on the value of A has shown that the nonnegligible values of A are mostly attributable to errors in estimating Z (Sathyendranath 1981). But remarkably high A values were observed for Emicort and Fos-Berre stations. Nonselectively absorbing particles of the type observed by Yentsch (1962) in the waters of Woods Hole could be responsible for high values of A , especially in coastal waters. Unfortunately, the absence of scattering data for the Emicort stations prevents a study of the relationship between A and P for this type of station. This problem is discussed in the section dealing with the relationship between $a(440)$ and Y' .

Table 3 summarizes the correlations between the measured parameters and the calculated coefficients. C is best correlated to C' rather than to any of the other coefficients. Equations 5a–d showed how this general correlation can be improved considerably when different types of waters are taken separately. As discussed earlier, the correlation between Y and Y' is not satisfactory. But Table 3 shows that this correlation is better than those between Y and the other coefficients. P is best correlated to P' , but there is also a significant correlation between P and Y' . This shows one of the problems of calculation. Since $a_p^{*'}(\lambda)$ and $a_y^{*'}(\lambda)$ are correlated in the region 400–570 nm ($r = 0.94$), the coefficients P' and Y' are correlated also ($r = 0.94$), and this in turn is responsible for the correlation between P and Y' . Thus, it is clear that calculating the coefficients will be easier when they can be calculated over the range 400–700 nm, which will reduce

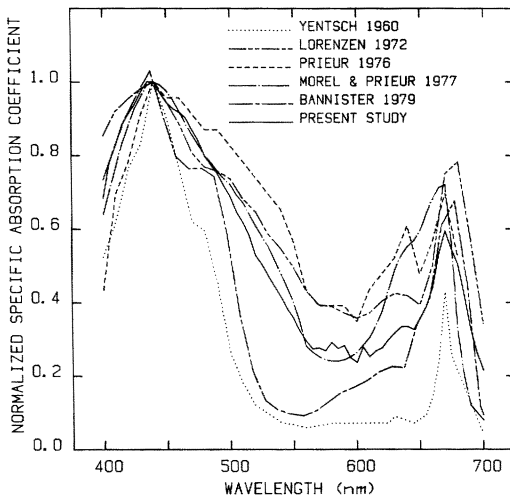


Fig. 7. Apparent specific absorption curve of phytoplankton pigments obtained in this study and some earlier results. All curves are normalized at 440 nm.

considerably the correlation of $a_p^{*'}(\lambda)$ with $a_y^{*'}(\lambda)$ as well as $a_c^{*'}(\lambda)$. But even in this range, $a_y^{*'}(\lambda)$ and $a_c^{*'}(\lambda)$ will still remain correlated ($r = 0.81$).

Discussion of the specific absorption curves

The $a_c^{*'}(\lambda)$ proposed in this study ought to be compared with the results of earlier studies. Prieur (1976) and Morel and Prieur (1977) used spectral data of a combined with measured phytoplankton concentrations to determine the in situ absorption curves of phytoplankton. But many others have measured the in vivo absorption curves of phytoplankton in laboratory cultures (Yentsch 1960; Lorenzen 1972; Duntley et al. 1974; Bannister 1979; Bricaud 1979; Kiefer et al. 1979). Figure 7 shows our results along with the results of some of the earlier studies, with all the curves normalized at 440 nm. The form of the mean curve proposed here does appear as an approximate mean of the earlier estimates, which show considerable diversity.

There is also strong disagreement about the absolute values of absorption per unit pigment concentration. Prieur (1976) and Morel and Prieur (1977) give 0.023 and $0.025 \cdot \text{m}^{-1} \cdot (\text{mg} \cdot \text{m}^{-3})^{-1}$ as the

value of in situ specific absorption by phytoplankton at 440 nm, but the laboratory experiments of Yentsch (1960) gave a value of 0.097 at the same wavelength. The specific absorption curve for an algal culture of *Chlorella pyrenoidosa* reported by Bannister (1979) has a value of 0.031 at 437.5 nm. The laboratory studies of Duntley et al. (1974), Bricaud (1979), and Kiefer et al. (1979) have shown that the absolute values are subject to change, depending on the type and physiological condition of the culture. Dubinsky and Berman (1979) reported an in situ specific irradiance attenuation coefficient, attributable to phytoplankton, of 0.012 at 450 nm; the corresponding specific absorption would be still less, since $a < K$. Earlier works cited above, which give specific irradiance attenuation coefficients for the whole visible region, also show considerable dispersion. The spectral values of the specific attenuation coefficient given by Smith and Baker (1978b) take the values 0.168 (when $C < 1$) and 0.039 (when $C > 1$) at 440 nm. According to our results (Eq. 5a, b, and d), the absolute increment per unit C can be 0.018 , 0.070 , and 0.077 , depending on the type of environment.

In fact, it is difficult to estimate how much of the observed variation of spectral forms or absolute values is really due to variations in the absorption characteristics of phytoplankton and how much to diversity of technique. Hardly any of the methods are comparable with each other or with those in the present study. The results of Morel and Prieur (1977) are based on a number of in situ measurements, but only two components (phytoplankton and all other substances) were considered responsible for absorption. Even if the same spectral data are used, the number of components chosen will influence the form of the specific absorption curve of phytoplankton, deduced by regression. Prieur (1976) used the values of $a(\lambda)$ at two stations and the corresponding values of C , Y , and b . In our method, the form of the curve is determined independently of these parame-

ters, which are only used to evaluate the absolute values of the specific absorption by regression. This has the advantage of reducing the influence of individual errors in the measurements. Laboratory measurements of phytoplankton absorption are made on cultures at very high concentrations (from 50 to $>1,000 \text{ mg Chl} \cdot \text{m}^{-3}$) and under conditions very different from those existing in the sea. These measurements are usually made with a spectrophotometer equipped with a diffuse absorption accessory (Duntley et al. 1974; Bannister 1979). The diversity even in such measurements can probably be attributed in part to diversity in the pigment composition of different phytoplankton species, since only the chlorophyll *a* concentration is taken into account in calculating specific absorption.

Besides this, comparison of these results assumes that Beer's law is applicable whatever be the concentration *C* and the nature of the cells containing the pigments. But Duysens (1956) and Kirk (1975*a,b*, 1976*a*) have demonstrated that the absorption curve of randomly and discretely distributed absorbing material shows a "flattening effect" when compared to the absorption curve of the same amount of pigments in a homogeneous solution. This effect depends on the size and form of the discrete absorbers and could also contribute to the diversity observed when different cultures are compared. It cannot be examined in detail here. However it is clear from examination of all these results that the specific absorption of phytoplankton is subject to a certain variability. Our study represents the first systematic effort to estimate the mean values of specific absorption *in situ*, applicable in studies of the effect of phytoplankton on the modification of the spectral composition of light penetrating the sea. Smith and Baker (1978*b*) made an analogous study, but of the diffuse attenuation coefficient, which is not the best parameter for this purpose, as we discuss below.

We used only three stations to calculate the $a_p^*(\lambda)$ curves, and we assumed

that the pigment concentrations at these stations were constant and equal to that at station 70 of Cineca V, which was not in fact strictly true (the *C* values varied from 1.7 to $2.4 \text{ mg} \cdot \text{m}^{-3}$ at these four stations). But the good correlation between *P* and *P'* appears to justify the approximation. Further studies should be carried out to determine the variability of this curve with location and season. The curve proposed here is based only on inshore stations of Cineca V, where resuspended inorganic detrital particles were responsible for most of the additional scattering and absorption observed (Morel 1981). However, this curve seems to apply equally well to our data from the other regions as far as reconstruction of the curves and relationship between *P* and *P'* are concerned. The left-hand side of the curve (Fig. 4) has a nearly exponential form similar to that of yellow substances and probably reflects the effect of this substance in colloidal or adsorbed form. Such an effect was also observed by Yentsch (1962) in particles from depths $>100 \text{ m}$. But our $a_p^*(\lambda)$ increased beyond 550 nm, whereas the absorption continued to decrease in the observations of Yentsch.

The optical classification

Several optical classifications have been proposed before. The best known and most widely used classification is that of Jerlov (1951), as slightly modified by him (Jerlov 1976). This remarkable classification, the first of its kind, has certain drawbacks, as has been pointed out by Pelevin and Rutkovskaya (1977) and Morel (1981). Jerlov's classification of coastal waters corresponds only to the J-type waters and cannot be used to classify U- or V-type. It is based on the diffuse attenuation coefficient, but under the specified conditions of measurements, this value is not very different from the absorption coefficient (Jerlov 1976). We have subjected the typical curves of Jerlov's classification to the component analysis presented here. Figure 8 shows the variations in the coefficients *C'*, *Y'*, *P'*, and *A* with variation in

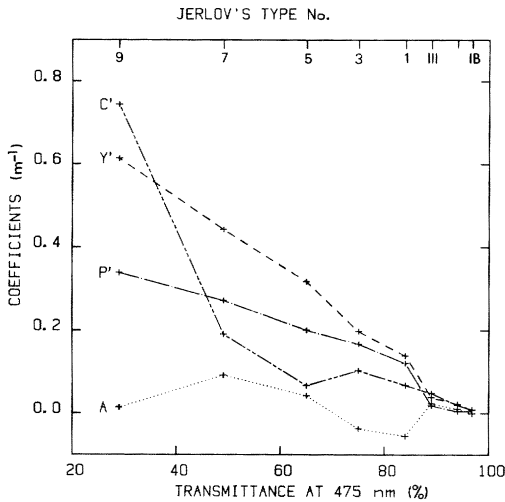


Fig. 8. Coefficients calculated for typical curves of Jerlov's classification. Coefficients are plotted as a function of transmittance at 475 nm. Type I and IA have negligible coefficients. "Oceanic" types IB to III and the "coastal" subtypes 1 to 9 are positioned in order from right to left.

water type, with transmittance at 475 nm as the index of the water type as defined by Jerlov. Obviously Y' plays the most systematic role in this classification; such an important contribution of yellow substances to the absorption coefficient is particular to the Baltic Sea and certain coastal waters and makes Jerlov's classification inapplicable to other regions. The modified nomogram proposed by Pelyin and Rutkovskaya (1977) is an improvement, because it rests on a statistical analysis of recently available data from the world oceans. Their suggestion that the diffuse attenuation coefficient at 550 nm be used as the continuous index of classification also overcomes the problem of discreteness in Jerlov's classification. But this classification becomes complicated if the observed spectra do not correspond to the form of the standard curves. Besides, this type of classification gives no insight into the factors which induce or influence the observed optical properties. The classification proposed by Smith and Baker (1978b) is a further improvement, since it separates the influence of phytoplankton pigments and the covarying substances on the diffuse at-

tenuation coefficient, but it becomes inapplicable in regions where the attenuation coefficient is highly influenced by resuspended sediments or terrigenous influx.

All these classifications are based on the diffuse attenuation coefficient, which is an easily measurable parameter but is not an inherent property of the water. We found (Eq. 2a) $K_d:a$ to vary from 1.05 to 1.7. This ratio is dependent on wavelength because it depends on R . It also depends on the radiance field, so there is a risk that the same water might be classified differently according to the conditions of measurements. In addition, the property of additivity is not applicable to K . For example, K_w , the diffuse attenuation coefficient of pure seawater, is often taken to be a constant (e.g. Smith and Baker 1978a,b). But the influence of pure seawater on K is not the same in water with high or low concentrations of phytoplankton, because the modification of the radiance field in the layer considered would not be the same in the two cases. That is to say, K_w changes with the amount of other absorbing and scattering material present in the water. Taking this variable parameter to be a constant would in turn affect the specific attenuation of the other absorbing agents obtained by regression.

The classification that we propose here is based on an inherent optical property of the water and the additivity of the absorption provoked by the different absorbing agents (Eq. 4a). Of the four calculated coefficients, C' and P' have been shown to be related to measured parameters. Theoretically, Y' , the coefficient corresponding to absorption by yellow substances, should be related to absorption in the UV region, for example at 350 nm, by Eq. 3. This measurement would be precise in waters with predominant absorption by yellow substances. The determination of Y' for the other waters is discussed below. The coefficient A has been inferred to be due to errors of measurement, except perhaps in certain special cases, and is therefore omitted from the general classification. We propose

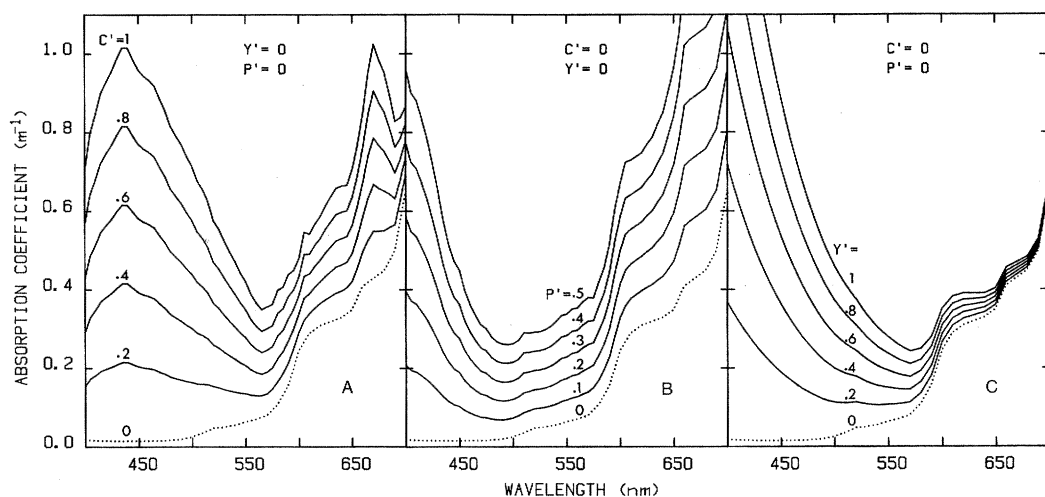


Fig. 9. Theoretical curves showing variations in absorption curve when absorption related to different quantities of any one of the coefficients C' , P' , and Y' (m^{-1}) is added to absorption due to pure seawater, while other coefficients are kept zero. Absorption due to pure seawater is shown in each panel by dotted lines. A. C' is changed progressively. B. P' is changed progressively. C. Y' is changed progressively.

that a given water type can be optically classified by the three coefficients C' , Y' , and P' . The spectral absorption curves can be reconstructed with little loss of detail by using these coefficients and their related specific absorption curves in the region from 400 to 570 nm and also in the range 570 to 700 nm, but with less precision in this region. The precision in this latter range can be improved when sufficient numbers of precise measurements become available in this region for improving the specific absorption curves proposed here, especially that of $a_p^*(\lambda)$. Figure 9 shows the variations in the absorption curves with changes in the coefficients C' , P' , and Y' ; these "pure" theoretical curves are slightly different from the observed curves in Fig. 1.

The relative importance of the three coefficients at the different stations is examined in Fig. 10A. Figure 10B proposes a nomenclature for the different types of water based on the predominant coefficients. The V-type stations fall in the C' -type. The curves of Jerlov's classification fall into the Y' -, $Y'P'$ -, and $Y'C'$ -types. Clear stations with very small coefficients are also observed to be of the C' -type. Very clear waters where the absorp-

tion curve is identical to absorption by water cannot be represented in this diagram because they have zero coefficients, but could be classified as W-type waters. The classification proposed here is similar to that of Kirk (1980) for inland waters, which separates the waters into type G (yellow substances or "gilvin"-dominated), type T (tripton-dominated), possibly a type A (phytoplankton-dominated), and various combinations of these basic types.

Applications

So far, we have discussed only the problems related to estimating the concentrations of dissolved and particulate matter in seawater, given the spectral absorption coefficient. But this calls for sophisticated optical instruments. The inverse problem, of calculating the spectral absorption coefficient, or of identifying the type of water from other parameters which can be routinely measured, will now be considered. Applications of our results in simple models of light penetration in seawater are also discussed.

Calculation of the absorption curves from C and b—The problems related to calculating Y' from Y have been dis-

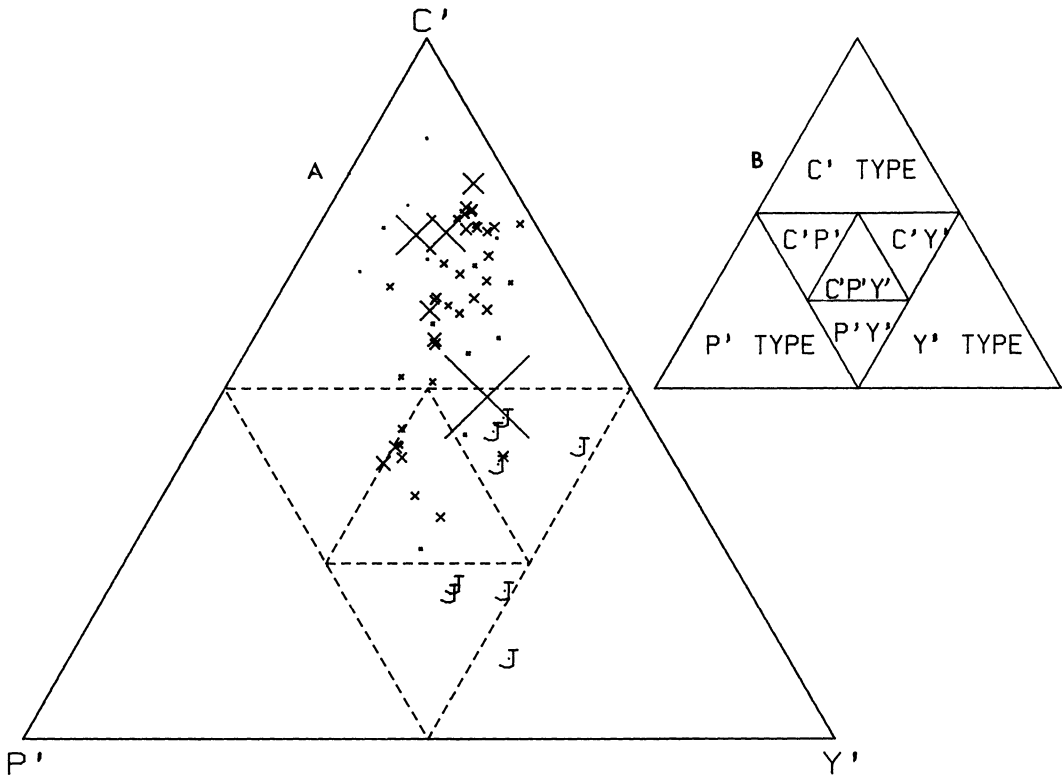


Fig. 10. Triangular diagram presenting proportions of C' , Y' , and P' in the sum of the three coefficients. A. Each station is represented by \times , the size of which is proportional to this sum. If any one coefficient is predominant, representative point will be close to corresponding vertex. Jerlov's types IB to 9 are indicated by J without size reference. B. Proposed mnemonic classification for different types of water based on predominant coefficients. For data at our disposal, contribution of phytoplankton pigments seems to be predominant. This is partly due to choice of 440 nm as wavelength of normalization, as it also corresponds to maximum of absorption by chlorophyll a . It will be hard to find the P' -type among oceanic waters, but such waters can probably be encountered in turbid inshore regions and inland water masses.

cussed. Fortunately, our results show a statistical relationship between $a(440)$ and Y' (Fig. 11) which is valid over two or three orders of magnitude and can be expressed as

$$Y'(\text{m}^{-1}) = -0.005 + 0.207a(440)(\text{m}^{-1}) \quad (9)$$

with $r = 0.99$ and $n = 55$. In this equation, $a(440)$ also includes $a_w(440)$. It is evident that this equation, which attributes about 20% of the total absorption at 440 nm to absorption by yellow substances, will not be applicable in regions such as the Baltic where yellow substances are the predominant absorbing agents.

Substituting Eq. 9 into 4b, we obtain

$$a(440)(1 - 0.207) = a_w(440) + C' + P' - 0.005. \quad (10)$$

Equations 5a, b, and d can be used to calculate C' , the choice depending on the nature of the waters investigated. P' can be calculated from Eq. 8, and then, $a(440)$ and Y' from Eq. 10 and 9. Thus, given C and b , the absorption curves can be calculated for these stations by also using Eq. 4a, if A is neglected. But the absorption curves calculated in this manner will show a constant offset from the measured absorption curves, its value determined by the value of A at the station. This offset can be important in the case of stations such as those of Emeric and

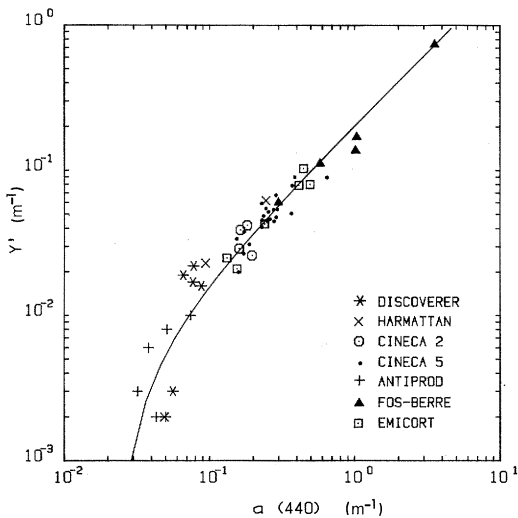


Fig. 11. $a(440)$ vs. Y' on a log-log scale. Curve is given by Eq. 9.

Fos-Berre. Figure 12 shows three examples of the absorption curves reconstructed in this manner. The observed absorption curves for the corresponding stations are also shown, for comparison, after subtracting the value of A . Comparison of the pairs of curves shows an average error of 12% and a maximum error of 25%. It is difficult to estimate how much of this increase in error is due to the problem of nonconcordance of the measurements discussed earlier.

Diagram quanta (%) – C, for diverse values of P' and Y' —This diagram (Fig. 13) can be used to estimate the optical parameters C' , P' , and Y' if the percentage energy in quanta at 5 m and the value of C are known, or, inversely, to estimate percentage quanta at 5 m from the optical parameters. To draw the nomogram, we first calculated $a(440)$ and Y' for given values of C' and P' , using Eq. 9 and 10. $a(\lambda)$ was then calculated by Eq. 4a from 400 to 700 nm. K_d was calculated by using Eq. 2 with 1.12 as the value of $1/\mu_d$. $R(\lambda)$ was estimated from the approximate formula given by Morel and Prieur (1977):

$$R(\lambda) = 0.33b_b(\lambda)/a \tag{11}$$

and b_b , the total scattering coefficient, can be calculated (see legend Fig. 13).

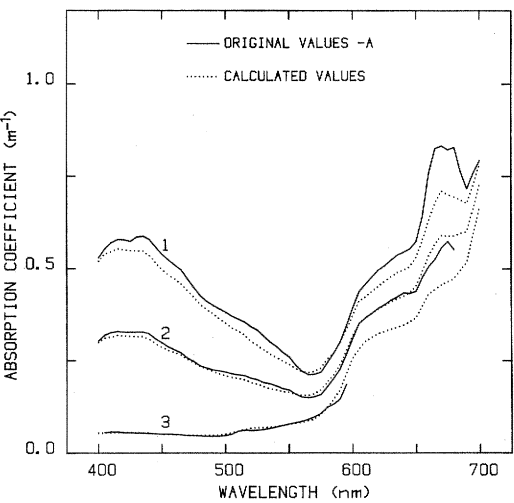


Fig. 12. Three examples of absorption curves estimated from values of C and b along with observed absorption curves at these stations from which coefficients A have been subtracted. 1—Station 71, Cineca V; 2—station 92, Cineca V; 3—station 10, Discoverer.

K_{\min} , the minimum attenuation at a single wavelength, was then determined. Using K_{\min} , we can easily calculate the relative energy E_{\max} (with respect to energy at the surface) at the corresponding wavelength for any given depth. Prieur and Caloumenos (1974) found a statistical relationship between the relative energy at the wavelength of spectral maximum, which is the same as E_{\max} , and the total energy in quanta, also in relative units (E_q), at a given depth. Therefore, E_q at 5 m can be calculated by using the equation given by Prieur and Caloumenos for 5 m:

$$\text{Log } E_q = 1.129 \text{ log } E_{\max} - 0.128. \tag{12}$$

The nomogram was constructed by repeating the calculations for different values of C' , P' , and Y' . The same nomogram can be constructed for different depths and by using alternate hypotheses in the intermediary steps.

When the number of intervening hypotheses in the construction of the nomogram is considered, the quantities estimated from it should be considered only rough approximations. The values of quanta (%) estimated from this nomo-

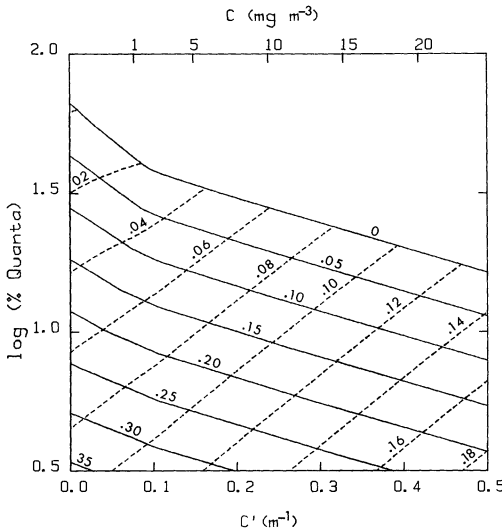


Fig. 13. Log of percentage of quantic energy at 5 m (with respect to energy at surface) as a function of C . Isolines of $P'(\text{m}^{-1})$ are shown by continuous lines and isolines of $Y'(\text{m}^{-1})$ by dashed lines. X-axis is also graduated in $C'(\text{m}^{-1})$ using Eq. 5a and b. $b_b(\lambda)$, necessary for calculation of $R(\lambda)$ (see Eq. 11), was expressed in form $b_b(\lambda) = r_w b_w(\lambda) + r_c b_c(\lambda) + r_p b_p(\lambda)$, which separates contribution of water, phytoplankton, and nonchlorophyllous particles. Each component of b_b is expressed as a product of total scattering coefficient b and corresponding back-scattering ratio $r = b_b:b$. The values of r_w (0.5), b_w at 500 nm ($0.0028 \cdot \text{m}^{-1}$), and the selectivity law ($\lambda^{-4.3}$) for b_w were taken from Morel (1974). $b_c(\lambda)$ and $b_p(\lambda)$ were fitted with a λ^{-1} selectivity. $b_c(550)$ and $b_p(550)$ are respectively b_{\min} and P (calculated from C' and P' by Eq. 5a, b, and 6). Suitable values of r_c and r_p were 0.005 and 0.02 (cf. Morel and Prieur 1977: $r = 0.005$ for V-type stations, $r = 0.015$ for U-type stations).

gram agreed with the observed values for some of our stations chosen to test its validity. In this diagram, Eq. 5a and b were used to transform C to C' and vice versa. For certain types of waters, a different relationship (e.g. Eq. 5d) will have to be used.

In primary production studies, since quanta and chlorophyll a concentrations are measured routinely, this nomogram could give an idea of the type of water studied without the necessity of determining P , Y , or $a(\lambda)$.

Relationship between percentage absorption by pure water and depth of the euphotic zone—The four coefficients and the normalized specific absorption curves,

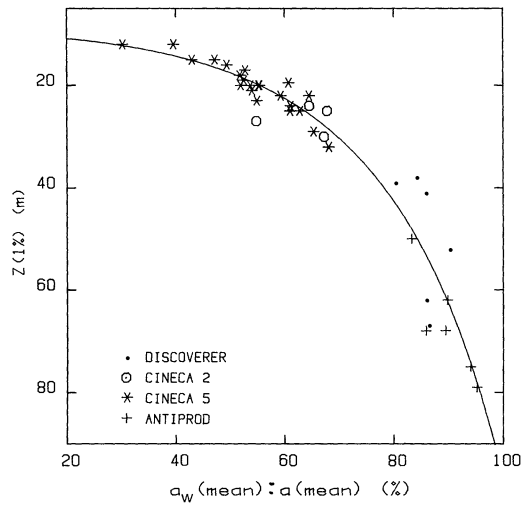


Fig. 14. Ratio of mean absorption due to water in the range 400–700 nm to mean absorption in this range, expressed in percentage, plotted against depth of euphotic zone, $Z(1\%)$.

along with the absorption curve of pure water, were used to calculate the absorption curve at all stations from 400 to 700 nm. The contribution of each component to the mean absorption in the visible region could then be calculated. Figure 14 shows a plot of the ratio of the mean absorption by pure water to the mean absorption coefficient (for the range 400–700 nm) vs. the depth of the euphotic zone, $Z(1\%)$. The correlation between these parameters is best expressed as

$$Z(1\%) = 9.966 \cdot \exp \left[0.00023 \left(\frac{a_w \text{ mean}}{a \text{ mean}} \% \right)^2 \right] \quad (13)$$

with $r = 0.97$ and $n = 38$. Thus, the depth of the euphotic zone can be estimated with good precision from the absorption values. The relationship of the percentage absorption due to other parameters with the euphotic zone is more complicated as they seem to depend on the water type; these relationships are not presented here.

Conclusion

The classification proposed here is based on the optical parameters C' , Y' ,

and P' , rather than their corresponding concentration units C , Y , and P given in Eq. 1. This was imposed by our results which showed that the relationship between C and C' depends on the nature of the waters considered. Our results have also brought out the differences between the measured concentration of yellow substances Y and the calculated parameter Y' . The importance of A , the constant coefficient, as a fourth parameter in certain waters needs to be investigated.

The method used here to calculate the normalized specific absorption curves of phytoplankton and inorganic particles is different from the classical methods of spectral analysis and was developed to make the best use of our data and obtain results easily interpretable from the physical point of view. The fact that the specific absorption curves were correlated among themselves necessitated the use of ridge regression, which gives a biased estimate of the coefficients; but despite this, the method has permitted simple modeling of spectral absorption in the sea, using routinely measurable parameters, with a good precision.

We stress that the specific absorption curve of phytoplankton proposed here is not identical to the specific absorption by pure chlorophyll a and pheophytin a . Besides the flattening effect due to the discrete random distribution of the absorbing centers in water, this curve also inevitably shows the influence of other coexisting pigments. But it does depict the form of the apparent absorption in the marine environment attributable to the presence of phytoplankton and for this reason should be very useful in models of radiative transfer. Similar reasoning also applies to absorption by nonchlorophyllous particulate matter.

The present treatment ignores the variability of the specific absorption curves of the three groups and so represents a first-order approximation of their true absorption. The spectral error in our reconstruction often falls within the precision of measurement, so that to take the variabilities into consideration would

call for more precise and extensive data than those at our disposal and a much more complicated mathematical approach. Even then, the resulting increase in accuracy of reconstruction would be of the order of only a few percent.

References

- BAIRD, I. E. 1973. Chlorophyll a and phaeopigments, p. C1–C25. Data Rep. Scripps Inst. Oceanogr. Ref. 73-16, v. 1.
- BANNISTER, T. T. 1979. Quantitative description of steady state, nutrient-saturated algal growth, including adaptation. *Limnol. Oceanogr.* **24**: 76–96.
- BAUER, D., AND A. IVANOFF. 1970. Spectro-irradiance-mètre. *Cah. Oceanogr.* **22**: 477–482.
- , AND ———. 1971. Description d'un diffusiomètre "intégrateur." *Cah. Oceanogr.* **23**: 827–839.
- BRICAUD, A. 1979. Absorption, diffusion (et rétro-diffusion) de la lumière par les substances influant sur la couleur des eaux de mer. Ph.D. thesis, 3rd cycle, Univ. Pierre et Marie Curie, Paris. 134 p.
- DUBINSKY, Z., AND T. BERMAN. 1979. Seasonal changes in the spectral composition of downwelling irradiance in Lake Kinneret (Israel). *Limnol. Oceanogr.* **24**: 652–663.
- DUNTLEY, S. Q., W. H. WILSON, AND C. F. EDGERTON. 1974. Ocean color analysis, part 1, p. 1.1–1.35. Visibility Lab. Scripps Inst. Oceanogr. Ref. 74-10.
- DUYSSENS, L. N. 1956. The flattening of the absorption spectra of suspensions as compared to that of solutions. *Biochem. Biophys. Acta* **19**: 1–12.
- HOERL, A. E., AND R. W. KENNARD. 1970a. Ridge regression: Biased estimation for non-orthogonal problems. *Technometrics* **12**: 55–67.
- , AND ———. 1970b. Ridge regression: Applications to non-orthogonal problems. *Technometrics* **12**: 69–82.
- HØJERSLEV, N. K. 1974. Inherent and apparent optical properties of the Baltic. Univ. Copenhagen Inst. Phys. Oceanogr. Rep. 23. 70 p.
- JACQUES, G. 1978. Données générales des stations, p. 19–33. Publ. CNEXO 16.
- , M. PANOUSE, AND J. GOSTAN. 1976. Répartition de la chlorophylle a et de la fluorescence, p. 1–10. Publ. CNEXO 10, Sect. 1.1.2.
- JERLOV, N. G. 1951. Optical studies of ocean water. Rep. Swedish Deep-Sea Exped. **3**: 1–59.
- . 1976. Marine optics. Elsevier.
- JONES, T. A. 1972. Multiple regression with correlated independent variables. *Math. Geol.* **4**: 203–218.
- KALLE, K. 1966. The problem of Gelbstoff in the sea. *Oceanogr. Mar. Biol. Annu. Rev.* **4**: 91–104.
- KIEFER, D. A., R. J. OLSON, AND W. H. WILSON. 1979. Reflectance spectroscopy of marine phytoplankton. Part 1. Optical properties as related

- to age and growth rate. *Limnol. Oceanogr.* **24**: 664–672.
- KIRK, J. T. 1975*a,b*. 1976*a*. A theoretical analysis of the contribution of algal cells to the attenuation of light within natural waters. 1. General treatment of suspensions of living cells. 2. Spherical cells. *New Phytol.* **75**: 11–20; 21–36. 3. Cylindrical and spheroidal cells. *New Phytol.* **77**: 341–358.
- . 1976*b*. Yellow substance (Gelbstoff) and its contribution to the attenuation of photosynthetically active radiation in some inland and coastal south-eastern Australian waters. *Aust. J. Mar. Freshwater Res.* **27**: 61–71.
- . 1980. The spectral absorption properties of natural waters: Contribution of the soluble and particulate fractions to light absorption in some inland waters of south-eastern Australia. *Aust. J. Mar. Freshwater Res.* **31**: 287–296.
- KOPELEVICH, O. V., S. Y. ROSANOV, AND I. M. NOSENKO. 1974. Light absorption by seawater, p. 107–112 [in Russian]. In A. S. Monin and K. S. Shifrin (eds.), *Hydrophysical and hydro-optical investigations in the Atlantic and Pacific Oceans*. Nauka, Moscow.
- LORENZEN, C. J. 1972. Extinction of light in the ocean by phytoplankton. *J. Cons. Cons. Int. Explor. Mer* **34**: 262–267.
- MARQUARDT, D. W. 1970. Generalized inverses, ridge regression, biased linear estimation, and non-linear estimation. *Technometrics* **12**: 591–612.
- MOREL, A. 1974. Optical properties of pure seawater, p. 1–24. In N. G. Jerlov and E. Steemann Nielsen (eds.), *Optical aspects of oceanography*. Academic.
- . 1980. In-water and remote measurements of ocean color. *Boundary-Layer Meteorol.* **18**: 177–201.
- . 1981. Optical properties and radiant energy in the waters of Guinea Dome and of Mauritanian upwelling area. Relation to primary productivity. *Rapp. P.V. Reun. Cons. Int. Explor. Mer* **180**, in press.
- , AND L. PRIEUR. 1975. Analyse spectrale des coefficients d'atténuation diffuse, d'absorption et de rétrodiffusion pour diverses régions marines. *Centre Rech. Oceanogr. Villefranche-sur-Mer Rapp.* **17**: 157 p.
- , AND ———. 1976. Analyse spectrale de l'absorption par les substances dissoutes (substances jaunes), p. 1–9. *Publ. CNEXO 10*, Sect. 1.1.11.
- , AND ———. 1977. Analysis of variations in ocean color. *Limnol. Oceanogr.* **22**: 709–722.
- , AND ———. 1978. Profils simultanés de la température et de la diffusion de la lumière dans la couche 0–100 mètres, p. 69–72. *Publ. CNEXO 16*.
- PELEVIN, V. N. 1965. Measurement of the true absorption coefficient of light in the sea. *Atm. Ocean Phy. Ser.* **1**: 539–545.
- , AND V. A. RUTKOVSKAYA. 1977. On the optical classification of ocean waters from the spectral attenuation of solar radiation. *Oceanology* **17**: 28–32.
- PREISENDORFER, R. W. 1961. Application of radiative transfer theory to light measurements in the sea. *Int. Geophys. Geod. Monogr.* **10**: 11–29.
- PRIEUR, L. 1976. Transfert radiatif dans les eaux de mer. Application à la détermination de paramètres optiques caractérisant leur teneur en substances dissoutes et leur contenu en particules. Ph.D. thesis, Univ. Pierre et Marie Curie, Paris. 243 p.
- , AND L. CALOUMENOS. 1974. Relations, pour l'éclairement sous-marin, entre la densité spectrale au voisinage de son maximum et le flux de photons entre 400 et 700 nm. *Ann. Inst. Oceanogr.* **50**: 127–137.
- , AND A. MOREL. 1971. Etude théorique du régime asymptotique. Relations entre caractéristiques optiques et coefficients d'extinction relatifs à la pénétration de la lumière du jour dans la mer. *Cah. Oceanogr.* **23**: 35–47.
- , AND ———. 1976. Mesures des coefficients de diffusion, d'atténuation et d'extinction (Atténuation "diffuse") à la longueur d'onde 546 nm, p. 1–257. *Publ. CNEXO 10*, Sect. 1.1.10.
- SATHYENDRANATH, S. 1981. Influence des substances en solution et en suspension dans les eaux de mer sur l'absorption et la réflectance. Modélisation et applications à la télédétection. Ph.D. thesis, 3rd cycle, Univ. Pierre et Marie Curie, Paris. 123 p.
- SAUBERER, F., AND F. RUTNER. 1941. Die Strahlungsverhältnisse der Binnengewässer. Becker and Erler, Leipzig. 240 p.
- SMITH, R. C., AND K. S. BAKER. 1978*a*. The bio-optical state of ocean waters and remote sensing. *Limnol. Oceanogr.* **23**: 247–259.
- , AND ———. 1978*b*. Optical classification of natural waters. *Limnol. Oceanogr.* **23**: 260–267.
- TYLER, J. E., AND R. W. PREISENDORFER. 1962. Transmission of energy within the sea, p. 397–451. In M. N. Hill (ed.), *The sea*, v. 1. Interscience.
- YENTSCH, C. S. 1960. The influence of phytoplankton pigments on the colour of sea water. *Deep-Sea Res.* **7**: 1–9.
- . 1962. Measurement of visible light absorption by particulate matter in the ocean. *Limnol. Oceanogr.* **7**: 207–217.

Submitted: 24 March 1980

Accepted: 21 January 1981